

## Synthesis, Biological Evaluation and in-silico investigations of Benzotriazole Derivatives as potential inhibitor of NIMA related kinase

Tahir Qadri<sup>a†</sup>, Mubashir Aziz<sup>b†</sup>, Pervaiz Ali Channar<sup>c</sup>, Mumtaz Hussain<sup>a</sup>, Syeda Abida Ejaz<sup>b\*</sup>, Hafiz Muhammad Attaullah<sup>b</sup>, Rabail Ujan<sup>d</sup>, Zahid Hussain<sup>a\*</sup>, Tasneem Zehra<sup>c</sup>, Aamer Saeed<sup>e</sup>, M.R.Shah<sup>f</sup>

<sup>a</sup>Department of Chemistry, University of Karachi, Karachi 75270, Pakistan

<sup>b</sup>Department of Pharmaceutical Chemistry, Faculty of Pharmacy, The Islamia University of Bahawalpur, Bahawalpur 63100, Pakistan

<sup>c</sup>Department of Basic Science and Humanities, Faculty of Information Science Humanities, Dawood University of Engineering and Technology Karachi 74800. Karachi

<sup>d</sup>Dr. M. A. Kazi Institute of Chemistry, University of Sindh, Jamshoro, Pakistan

<sup>e</sup>Department of Chemistry, Quaid-I-Azam University, Islamabad 45320, Pakistan

Corresponding authors

<sup>f</sup>H.E.J.research institute of chemistry, international center for chemical and biological sciences, university of Karachi, Karachi 7527, Pakistan.

†these authors have contributed equally to this work

### \*Corresponding authors

Dr. Syeda Abida Ejaz

[abida.ejaz@iub.edu.pk](mailto:abida.ejaz@iub.edu.pk)

Zahid Hussain

[zahidhussain@uok.edu.pk](mailto:zahidhussain@uok.edu.pk)

### Hirshfeld surface analysis

In order to visualize the intermolecular interactions in the crystal of the title compound, (I), a Hirshfeld surface (HS) analysis (Hirshfeld, 1977; Spackman & Jayatilaka, 2009) was carried out by using *Crystal Explorer 17.5* (Turner et al., 2017). In the HS plotted over  $d_{\text{norm}}$  (Fig. 1), the white surface indicates contacts with distances equal to the sum of van der Waals radii, and the red and blue colours indicate distances shorter (in close contact) or longer (distinct contact) than the van der Waals radii, respectively (Venkatesan et al., 2016). The shape-index of the HS is a tool to visualize the  $\pi \dots \pi$  stacking by the presence of adjacent red and blue triangles; if there are no adjacent red and/or blue triangles, then there are no  $\pi \dots \pi$  interactions. Fig. 2 clearly suggests that there are no  $\pi \dots \pi$  interactions in (I). The overall two-dimensional fingerprint plot, Fig. 4a, and those delineated into H ... H, H ... C/C ... H, H ... N/N ... H, C ... N/N ... C, C ... C and H ... O/O ... H (McKinnon et al., 2007) are illustrated in Figs. 3 b–g, respectively, together with their relative contributions to the Hirshfeld surface. The most important interaction is H ... H contributing 67.3% to the overall crystal packing, which is reflected in Fig. 3b as widely scattered points of high density due to the large hydrogen content of the molecule with the tip at  $d_e = d_i = 1.13 \text{ \AA}$ . The pair of characteristic wings in the fingerprint plot delineated into H ... C/C ... H contacts (Fig. 3c, 21.9% contribution to the HS) has the tips at  $d_e + d_i = 2.68 \text{ \AA}$ . The pairs of wings resulting in the fingerprint plot delineated into H ... N/N ... H, Fig. 3d, contacts with 6.6% contribution to the HS are viewed with the tips at  $d_e + d_i = 2.27 \text{ \AA}$  and  $d_e + d_i = 2.70 \text{ \AA}$  for the

long and the short spikes, respectively. The pairs of C ... N/N ... C (Fig. 3e) and C ... C (Fig. 3f) contacts have contributions of 2.2% and 1.5% to the HS, and they are viewed with the tiny tips at  $d_e + d_i = 3.42 \text{ \AA}$  and  $d_e + d_i = 3.40 \text{ \AA}$ , respectively. Finally, the H ... O/O ... H (Fig. 3g) contacts with 0.5% contribution to the HS have distributions of the scattered points of very low density.

The Hirshfeld surface representations with the function  $d_{\text{norm}}$  plotted onto the surface are shown for the H ... H and H ... C/C ... H interactions in Figs. 4 a and b, respectively.

The Hirshfeld surface analysis confirms the importance of H-atom contacts in establishing the packing. The large number of H ... H and H ... C/C ... H interactions suggest that van der Waals interactions and hydrogen bonding play the major roles in the crystal packing (Hartwar et al., 2015).

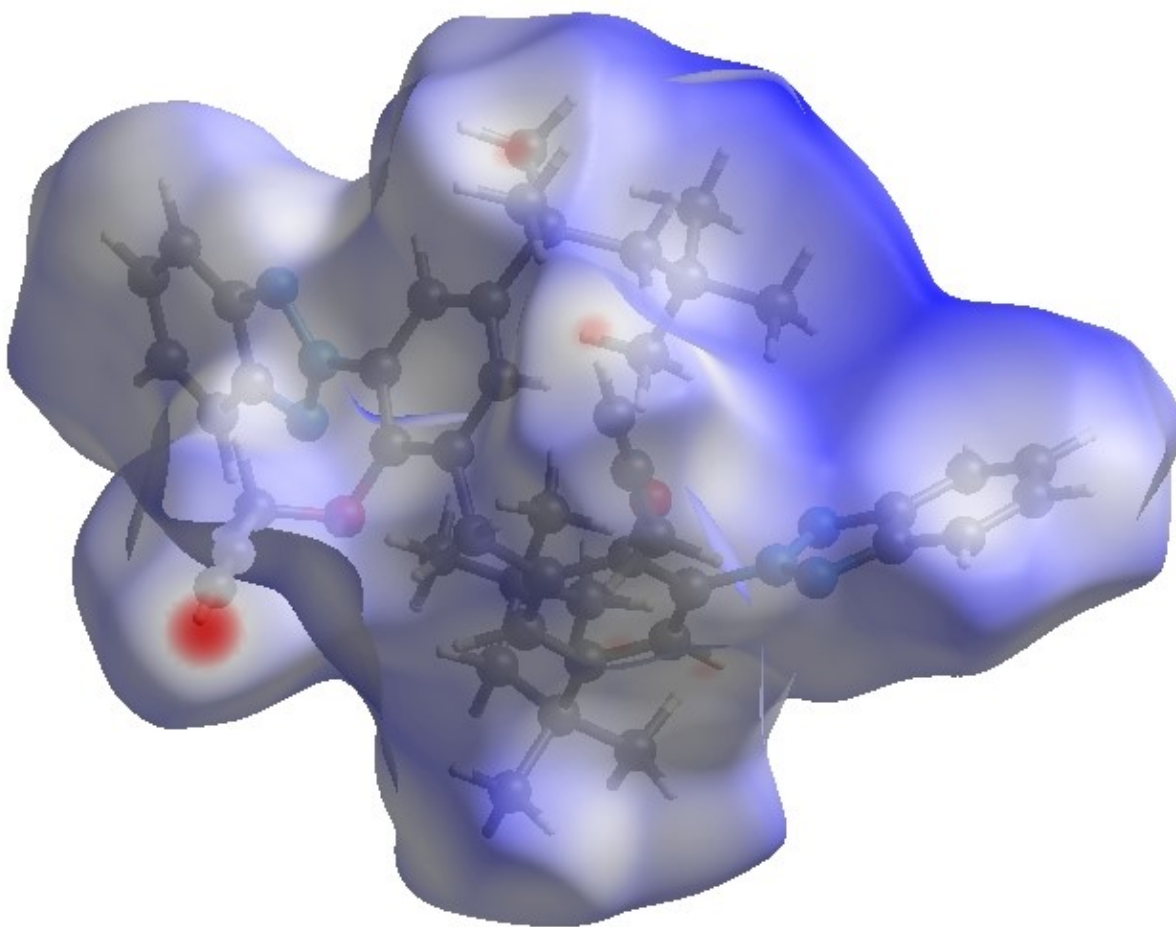


**Figure S1.** View of the three-dimensional Hirshfeld surface of the title compound plotted over  $d_{\text{norm}}$  in the range of  $-0.2851$  to  $2.3624$  a.u.

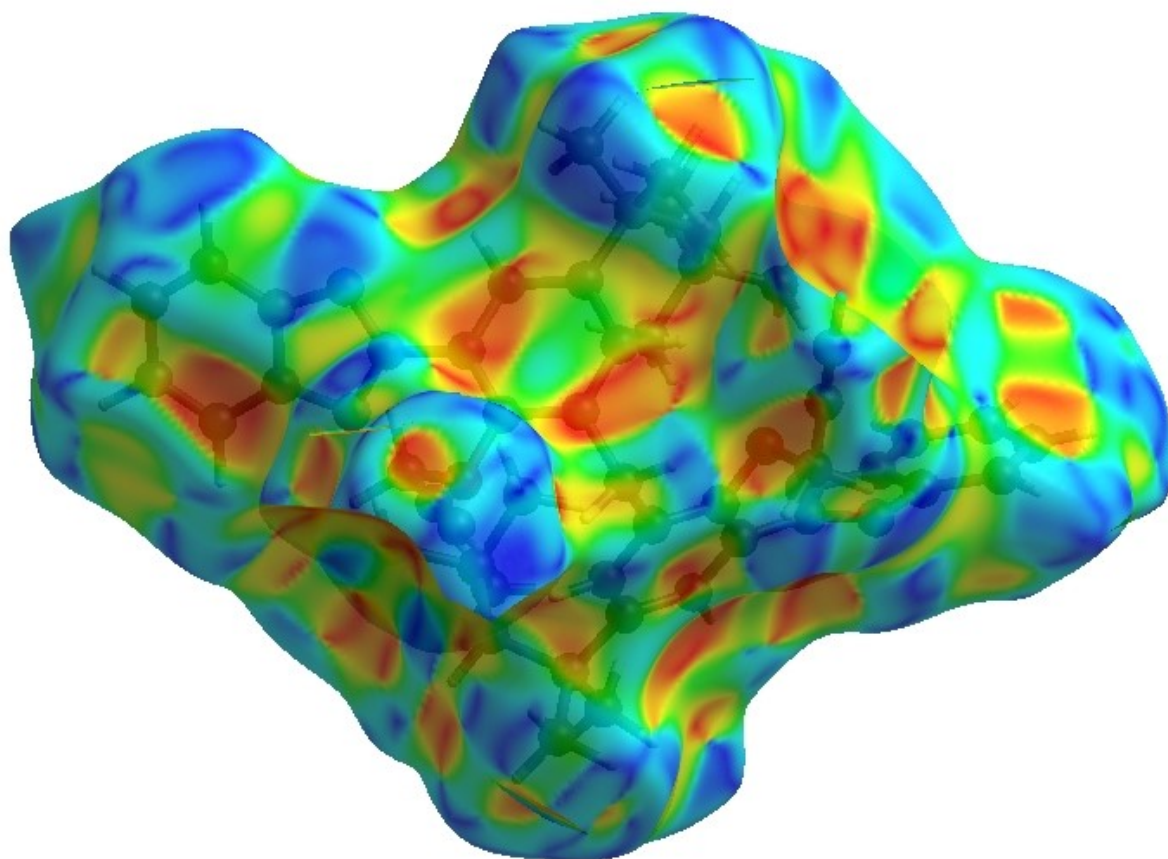


**Figure S2.** Hirshfeld surface of the title compound plotted over shape-index.

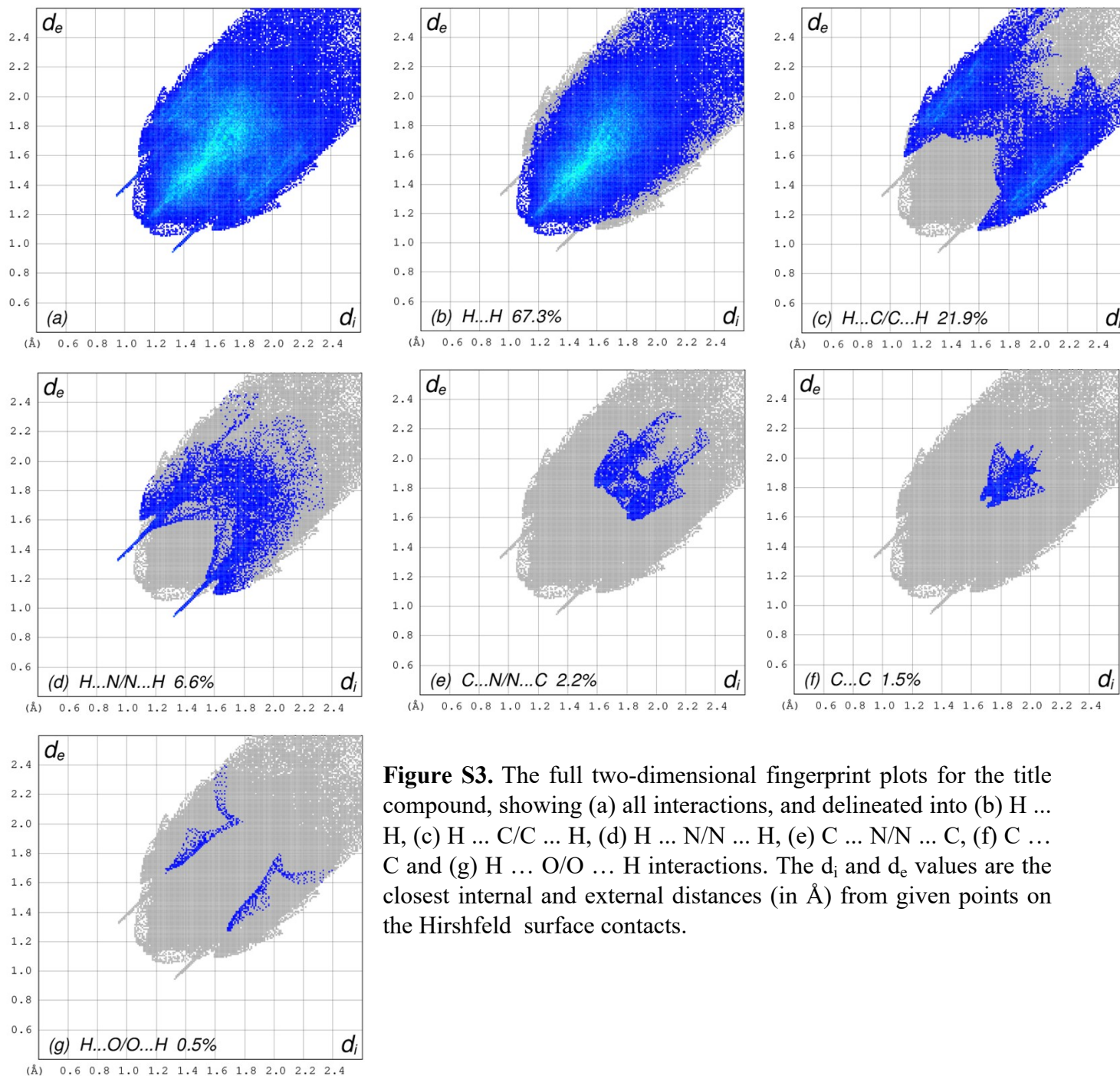
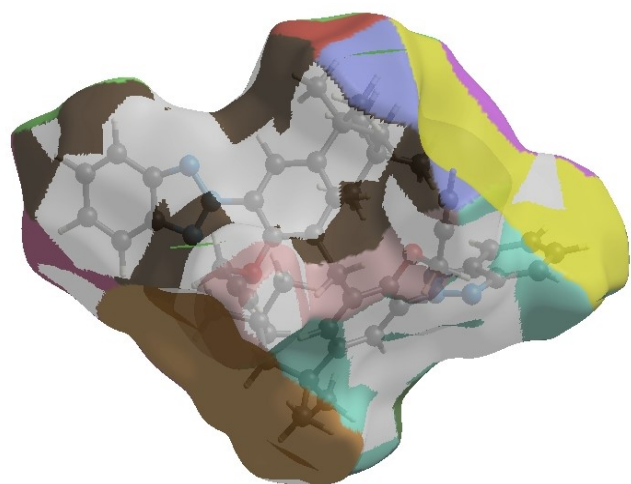
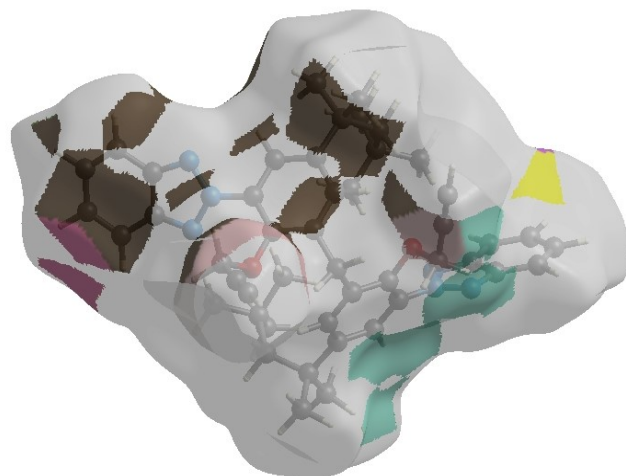


**Figure S3.** The full two-dimensional fingerprint plots for the title compound, showing (a) all interactions, and delineated into (b) H ... H, (c) H ... C/C ... H, (d) H ... N/N ... H, (e) C ... N/N ... C, (f) C ... C and (g) H ... O/O ... H interactions. The  $d_i$  and  $d_e$  values are the closest internal and external distances (in Å) from given points on the Hirshfeld surface contacts.



(a)



(b)

**Figure S4.** The Hirshfeld surface representations with the function  $d_{\text{norm}}$  plotted onto the surface for (a) H ... H and (b) H ... C/C ... H interactions.

**Table S1. Experimental details.**

Crystal data	
Chemical formula	$C_{47}H_{54}N_6O_2$
$M_r$	734.96
Crystal system, space group	Triclinic, $P-1$
Temperature (K)	100
$a, b, c$ (Å)	11.4805 (4), 13.8247 (4), 14.6180 (6)
$\alpha, \beta, \gamma$ (°)	104.808 (3), 103.706 (3), 100.642 (3)
$V$ (Å <sup>3</sup> )	2103.58 (14)
$Z$	2
Radiation type	Mo $K\alpha$
$\mu$ (mm <sup>-1</sup> )	0.07
Crystal size (mm)	0.30 × 0.25 × 0.20
Data collection	
Diffractometer	Agilent SuperNova Dual diffractometer with an Atlas detector
Absorption correction	Multi-scan ( <i>CrysAlis PRO</i> ; Agilent, 2010)
$T_{\min}, T_{\max}$	0.822, 1.000
No. of measured, independent and observed [ $I > 2\sigma(I)$ ] reflections	17578, 9290, 6994
$R_{\text{int}}$	0.031
$(\sin \theta/\lambda)_{\text{max}}$ (Å <sup>-1</sup> )	0.650
Refinement	
$R[F^2 > 2\sigma(F^2)], wR(F^2), S$	0.051, 0.127, 1.01
No. of reflections	9290
No. of parameters	514
No. of restraints	2
H-atom treatment	H atoms treated by a mixture of independent and constrained refinement
$\Delta\rho_{\text{max}}, \Delta\rho_{\text{min}}$ (e Å <sup>-3</sup> )	0.47, -0.30

Computer programs: *CrysAlis PRO* (Agilent, 2010), *SHELXS97* (Sheldrick, 2008), *SHELXL97* (Sheldrick, 2008), *X-SEED* (Barbour, 2001), *pubCIF* (Westrip, 2010).

**Table S2. Hydrogen-bond geometry (Å, °).**

$D-H\cdots A$	$D-H$	$H\cdots A$	$D\cdots A$	$D-H\cdots A$
C41—H41 <sup>i</sup> ⋯N3 <sup>i</sup>	0.96 (1)	2.38 (1)	3.283 (3)	158 (2)

Symmetry code: (i) x-1, y, z.

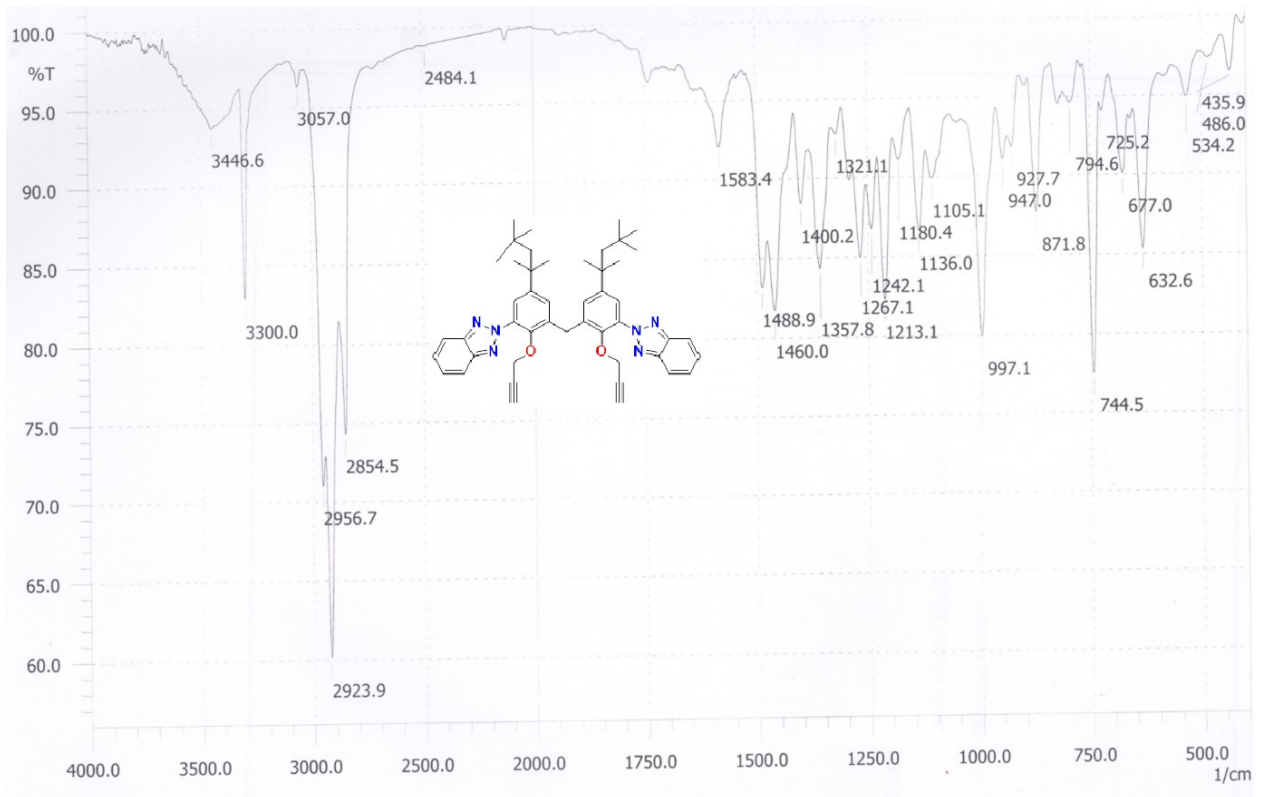


**Figure S5.  $C^{13}$ -NMR spectra of TAJ1**

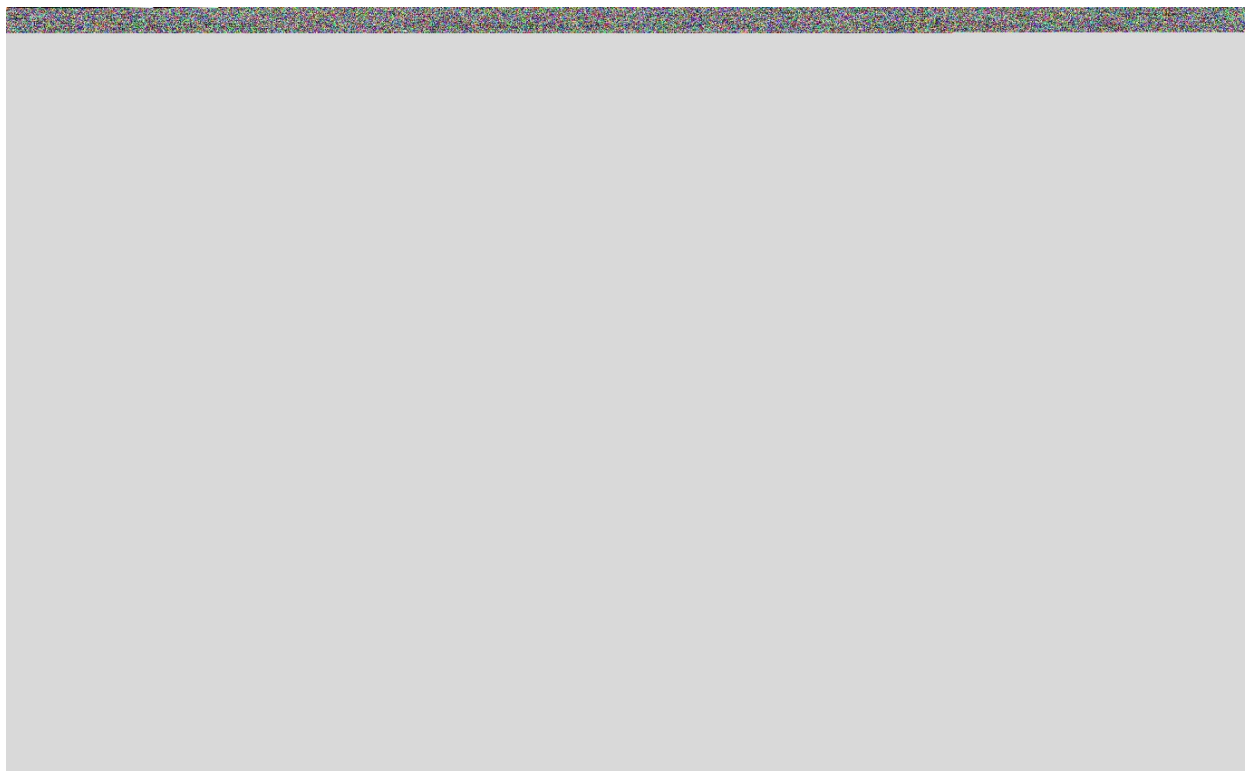


**Figure S6.  $C^{13}$ -NMR spectra of TAJ1**

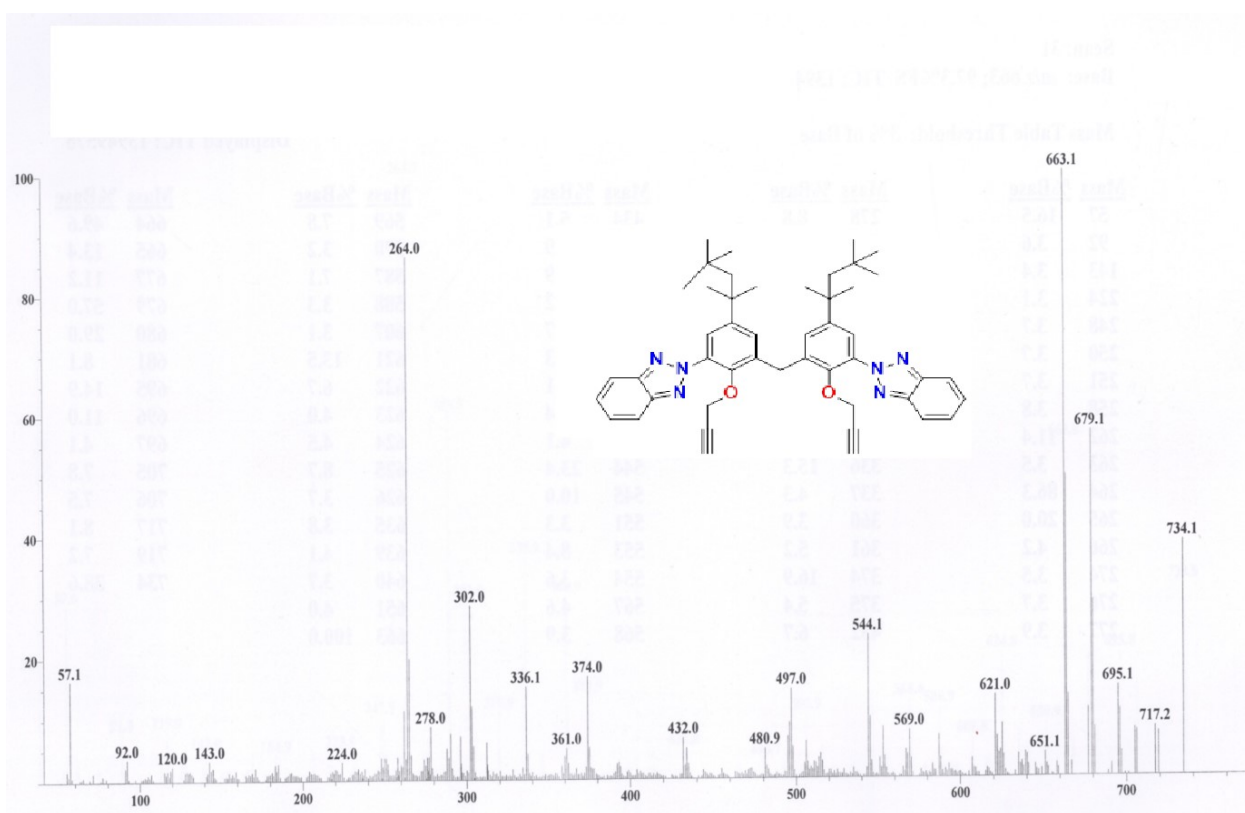


## Figure S7. HNMR spectra of TAJ1

### Molecular Dynamics Simulation

Molecular Dynamics simulation was performed in duplet in order to enhance the reliability of the simulated findings. It was observed that all three simulated complex revealed almost similar pattern as that of main production run. The average RMSD of NEK7-TAJ1 complex was 2.2 angstroms, NEK2-TAJ1 complex was at 3.2 angstroms and tP53-TAJ1 complex simulated with average RMSD of 4.6 angstroms respectively. All these findings further validate the in-vitro and in-silico investigations. Replica MD simulation is illustrated in Figure S8.

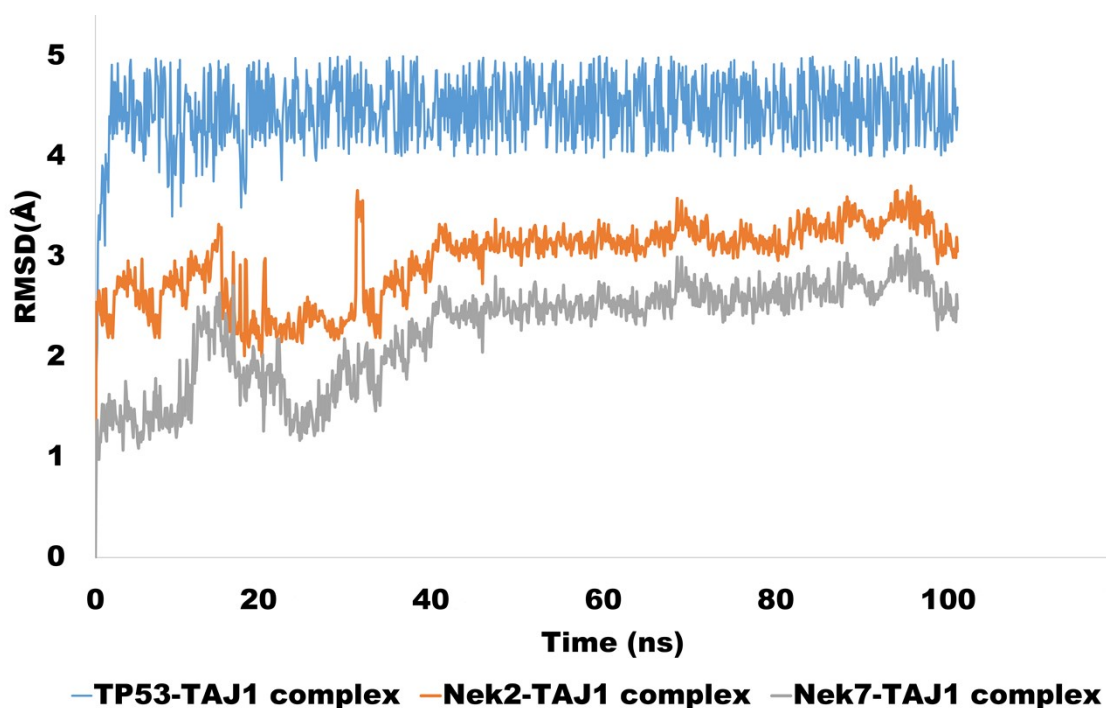


Figure S8. Second replica of MD simulation for selected complexes.

### References:

Agilent Technologies (2010). CrysAlis PRO. Yarnton, Oxfordshire, England.

Hartwar, V. R.; Sist, M.; Jorgensen, M. R. V.; Mamakhel, A. H.; Wang, X.; Hoffmann, C. M.; Sugimoto, K.; Overgaard, J.; Iversen, B. B. *Quantitative analysis of intermolecular interactions in orthorhombic rubrene*. *IUCrJ* **2015**, 2, 563—574.

Hirshfeld, F. L. *Bonded-Atom Fragments for Describing Molecular Charge Densities*. *Theor. Chim. Acta* **1977**, 44, 129—138.

McKinnon, J. J.; Jayatilaka, D.; Spackman, M. A. *Towards quantitative analysis of intermolecular interactions with Hirshfeld surfaces*. Chem. Commun. **2007**, 3814—3816.

Sheldrick, G. M. Acta Cryst. **2015**, C71, 3-8.

Spackman, M. A.; Jayatilaka, D. *Hirshfeld surface analysis*. CrystEngComm. **2009**, 11, 19—32.

Turner, M. J.; McKinnon, J. J.; Wolff, S. K.; Grimwood, D. J.; Spackman, P. R.; Jayatilaka, D.; Spackman, M. A. (2017). *CrystalExplorer17*. The University of Western Australia.

Venkatesan, P.; Thamotharan, S.; Ilangovan, A.; Liang, H.; Sundius, T. *Crystal structure, Hirshfeld surfaces and DFT computation of NLO active (2E)-2-(ethoxycarbonyl)-3-[(1-methoxy-1-oxo-3-phenylpropan-2-yl)amino] prop-2-enoic acid*. Spectrochim. Acta Part A **2016**, 153, 625—636.